FINAL REPORT

on

STRENGTH ANALYSIS OF BRITTLE MATERIALS

to

OFFICE OF NAVAL RESEARCH
Contract No. N00014-73-C-0408, NR 032-541

November, 1977

by

G. K. Bansal, W. H. Duckworth, and D. E. Niesz

BATTELLE
Columbus Laboratories
505 King Avenue
Columbus, Ohio 43201

FINAL REPORT

on

STRENGTH ANALYSIS OF BRITTLE MATERIALS

to

OFFICE OF NAVAL RESEARCH
Contract No. N00014-73-C-0408, NR 032-541

November, 1977

by

G. K. Bansal, W. H. Duckworth, and D. E. Niesz

BATTELLE
Columbus Laboratories
505 King Avenue
Columbus, Ohio 43201

TABLE OF CONTENTS

TABLE OF CONTENTS (Continued)

LIST OF FIGURES

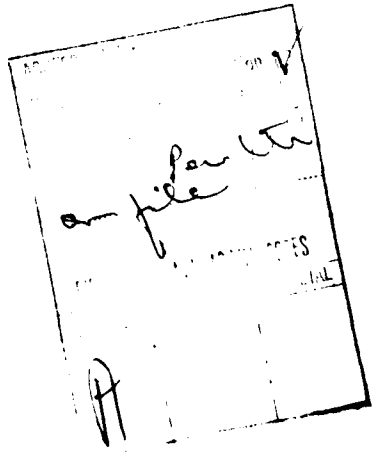

LIST OF TABLES

STRENGTH ANALYSIS OF BRITTLE MATERIALS

by

G. K. Bansal, W. H. Duckworth, and D. E. Niesz

INTRODUCTION

This final report summarizes research for the Office of Naval Research under Contract No. N00014-73-C-0408, and performed in the period from April, 1973, to September, 1977.

This research was directed to characterizing and explaining strength-size relations exhibited by ceramic materials in the interest of establishing a structural design technology for these materials. Four commercial polycrystalline ceramics of importance for Navy structural uses were studied.

RESEARCH ACCOMPLISHMENTS

Accomplishments under the contract are reported in the 12 publications* listed in Table 1 and the five technical reports listed in Table 2. Manuscripts are being prepared for two additional publications whose titles are also given in Table 1.

One of the publications, "Effects of Specimen Size on Ceramic Strengths", summarizes the major research thrust and is included as Appendix A of this report.

An important result of the research was its contribution to ceramic structural design technology. This contribution, on treating size dependence in obtaining failure criteria, has been incorporated in another of the publications, "Structural Designing With Ceramic Materials" which is reproduced as Appendix B of this report.

The research required extensive ceramographic work, and accomplishments in this area resulted in the four technical awards listed in Table 3.

* Eight published and four accepted for publication.

TABLE 1. TECHNICAL PUBLICATIONS

(1) "Effect of Flaw Shape on Strength of Ceramics", J. Am. Ceram. Soc., 59 [1-2] 87-88 (1976).

(2) "Reduction of Errors in Ceramic Bend Tests", J. Am. Ceram. Soc., 59 [5-6] 189-92 (1976).

(3) "Strength-Size Relationships in Ceramic Materials: Investigation of a Commercial Glass-Ceramic", Am. Ceram. Soc. Bull., 55 [3] 289-92, 307 (1976).

(4) "Strength-Size Relations in Ceramic Materials: Investigation of an Alumina Ceramic", J. Am. Ceram. Soc., 59 [11-12] 472-78 (1976).

(5) "Comments on Griffith Fracture Equation - An Experimental Test", J. Appl. Phys. 47 [6] 2761 (1976).

(6) "On Fracture Mirror Formation in Glass and Polycrystalline Ceramics", Phil. Mag. 35 [4] 935-44 (1977).

(7) "Effects of Ceramic Microstructure on Strength and Fracture Surface Energy", pp 860-71 in Ceramic Microstructure 76, edited by R. M. Fulrath and J. A. Pask, Westview Press, Boulder, Colorado (1977).

(8) "Fracture Stress as Related to Flaw and Fracture Mirror Sizes", J. Am. Ceram. Soc., 60 [7-8] 304-10 (1977).

(9) "Effects of Moisture-Assisted Slow Crack Growth on Ceramic Strength", J. Mat. Sc. (accepted for publication).

(10) "Comments on Subcritical Crack Extension and Crack Resistance in Polycrystalline Alumina", J. Mat. Sc (accepted for publication).

(11) "Effects of Specimen Size on Ceramic Strengths", Proc. Fracture Mechanics of Ceramics (1977), (accepted for publication).

(12) "Structural Designing with Ceramic Materials", J. Am. Soc. Mech. Engr. (accepted for publication).

Two additional manuscripts are being prepared as follows:

(1) Strength-Size Relationships in a Hot-Pressed Alumina.

(2) Strength-Size Relationships in a Hot-Pressed Silicon Nitride.

TABLE 2. TECHNICAL REPORTS

(1) Reduction of Errors in Ceramic Bend Tests (July, 1974).

(2) Characteristics of Spray-Dried Granules as Related to Control of Ceramic Strength Behavior (August, 1974).

(3) Strength-Size Relationships in Ceramic Materials: Investigation of Pyroceram 9606 (November, 1974).

(4) (a) Strength-Size Relationships in Ceramic Materials: Investigation of a Commercial Alumina (October, 1975).

(b) Effect of Flaw Shape on Strength of Ceramics (October, 1975).

(5) Fracture Stress as Related to Flaw and Fracture Mirror Sizes in Two Polycrystalline Ceramics (May, 1976).

TABLE 3. AWARDS

Four awards were received in three different contests, as follows:

(1) "Identification of Strength-Controlling Flaws in Polycrystalline Ceramics Using Scanning Electron Fractography", Best in Show and First in Class, Ceramographic Exhibit (1976), American Ceramic Society.

(2) "Model for Macrocrack Propagation in Ceramic Polycrystals", Third in Class, Ceramographic Exhibit (1977), American Ceramic Society.

(3) "Macro-Fracture Analysis of Strength-Controlling Flaws in Polycrystalline Ceramics Using Stereo Fractography", Honorable Mention, International Metallographic Exhibit (1976), American Society of Metals.

(4) "Model for Macrocrack Propagation in Ceramic Polycrystals", Honorable Mention, International Metallographic Exhibit (1976), American Society of Metals.

SUMMARY

The four ceramics studied were a glass-ceramic, a conventionally sintered Al_2O_3, a hot-pressed Al_2O_3, and a hot-pressed Si_3N_4. Two sizes of specimens of each ceramic were investigated. They differed in each linear dimension by a factor of four or five and were cut from the same or like billets and finish ground identically. Fracture stress in each specimen was determined in a carefully controlled bend test at room temperature. The effective size of small specimens was altered in testing by the use of both 3- and 4-point loading. Variation in the extent of subcritical crack growth was obtained by conducting tests in either of two environments, dry N_2 or water. After testing, fracture surfaces were examined by optical and stereo scanning electron microscopy, particularly to characterize fracture-initiating flaws.

Qualitatively, mean strengths decreased with specimen size and strengths of individual specimens of the same size were dispersed, except in the case of glass-ceramic specimens tested in water. Investigation indicated that variable severity of fracture-initiating flaws was the sole factor responsible for strength variations in the following cases:

- glass-ceramic specimens tested in dry N_2
- sintered Al_2O_3 specimens tested in both dry N_2 and water
- hot-pressed Al_2O_3 specimens tested in dry N_2.

The water-tested glass-ceramic specimens, which did not exhibit a size effect nor significant dispersion of individual strength values, failed from flaws of uniform severity. The critical stress-intensity factor, K_{IC}, of the hot-pressed Al_2O_3 tended to increase with the extent of subcritical crack growth that preceded fracture when specimens were tested in water. Also there was evidence that the K_{IC} governing fracture in Si_3N_4 specimens varied inconsistently among specimens.

Fractographic examinations revealed the presence of at least two distinctly different types of fracture initiating flaws in each ceramic except the hot-pressed Si_3N_4.

In dry-N_2 tests of the glass-ceramic, machining-induced surface flaws were responsible for high-stress failures and sparsely distributed pores were responsible for low-stress failures. Subcritical crack growth from the machine flaws was found responsible for all fracture origins in water tests. Because of either their uniform size or dense population in the surface, or both, the machine flaws did not introduce an effect of size on strength within the limit of specimen sizes investigated either in dry-N_2 tests or after uniform subcritical growth during testing in water*. Low-stress, pore-initiated fracture occurred more frequently with increased specimen size in the dry-N_2 tests simply because of the greater likelihood of a pore being present in the larger volume subjected to tension. As a consequence, mean strengths decreased with specimen size. Pore-initiated failures were absent in specimens tested in water because of the increased severity of surface flaws apparently without change in the severity of pores. Billet-to-billet microstructural differences imposed specimen limitations that prevented a quantitative statistical characterization of strength of the glass-ceramic specimens. It is clear, however, that the strength distribution would be bimodal, exhibiting a low-stress regime where pores control failure and the failure probability as a function of stress is volume dependent. At higher stresses, the data suggest that the probability of failure would be negligible and size independent until the machine-flaw-controlled fracture stress is reached.

Effects from more than one flaw population and a variable K_{IC} were absent in the following sets of strength data reflecting size dependencies:

- All three effective sizes of sintered-Al_2O_3 specimens tested in water, representing failure stresses from $\sim$240 to 310 MN/m^2.
- 3- and 4-point, small sintered-Al_2O_3 specimens tested in dry N_2, representing failure stresses from $\sim$335 to 425 MN/m^2.

* The strength in water calculated from the dry-N_2 strength agreed closely with that observed. The calculation was based on a separate determination of the rate of subcritical crack growth in water as a function of stress-intensity factor. This finding indicates that the identical machine flaws were responsible for both subcritical crack growth in water and critical crack growth in dry N_2.

- 3- and 4-point, small hot-pressed Al_2O_3 specimens tested in dry N_2, representing failure stresses from $\sim$660 to 930 MN/m^2.

The research indicated applicability of Weibull statistics to each of these three sets of data. Specifically, for each set of data a single two-parameter Weibull function described the relation between failure probability (P) and failure stress (σ), and the predicted effects of size on each P-σ relation agreed with those observed. Fractographically observed surface flaws were responsible for all failures in the three sets of data, and Weibull's surface integral rather than his volume integral was applicable in determining the size dependence. In sum, merit was established for the following relation in describing each of these three sets of strength data:

$$P = 1 - \exp \left[- \int_S (\sigma/\sigma_o)^m \, dS \right]$$

where S is effective surface area, m is the Weibull modulus and σ_o is a normalizing constant.

In tests of both sintered and hot-pressed alumina's in dry N_2, a different flaw population controlled failure in large specimens than that in the small 3- and 4-point specimens discussed above. These flaws were generally more severe and ranged more in severity than the flaws responsible for fracture in the small specimens, and they were not necessarily located in the surface. The lower range of strengths exhibited by the large specimens gave P-σ relations that also could reasonably be described by two-parameter Weibull functions. Weibull moduli for the large specimens were 11 and 9 for the sintered and hot-pressed Al_2O_3, respectively, in contrast to 34 and 17 for the small specimens. The lower Weibull moduli were applicable to failures in the following stress ranges:

- Sintered Al_2O_3: $\sim$ 250 to 335 MN/m^2
- Hot-pressed Al_2O_3: $\sim$ 400 to 575 MN/m^2.

Since failures in these stress ranges were observed only in large specimens, it was not possible to evaluate size-effect predictions for their occurrence, except to note that the nature of the fracture-initiating flaws suggested a volume rather than surface integral to account for the size dependence. The important point, however, is that, like the glass-ceramic, both the sintered and hot-pressed Al_2O_3 are at least bimodal in their strength behavior in dry N_2, so P-σ relations of neither material could be described by a single set of Weibull parameters for the entire range of observed strengths.

The same Weibull function described the strength data from tests of small sintered Al_2O_3 specimens in dry N_2 and water, and fracture in these specimens resulted from surface flaws. These facts suggest that the identical flaws were responsible for initiating subcritical crack growth in water and critical growth in dry N_2. This indication was supported by other evidence. Specifically, mean strengths in water calculated from mean strengths in dry N_2 agreed closely with those measured. The calculation required a separate determination of the rate of subcritical crack growth in water as a function of stress intensity factor.

As noted above, strengths of the hot-pressed Al_2O_3 specimens were dependent on specimen size and no single Weibull function was adequate in describing strength dispersions over the entire range of observed strength values. In addition to two or more flaw populations being present, K_{IC} also varied among specimens of this material tested in water. The variation occurred in a consistent manner, increasing with the extent of subcritical crack growth. In this case, the effect of variable K_{IC} on strength must be determined independently and strength values adjusted accordingly prior to any statistical treatment of the data to define the size dependence of its strength.

In the hot-pressed silicon nitride, no fractographic evidence of more than one flaw population was found, but observed strength dispersions for specimens having different effective sizes could not be described clearly by one Weibull function. The reason was not firmly established, but evidence of a variable K_{IC} in the material was found.

APPENDIX A

EFFECTS OF SPECIMEN SIZE ON CERAMIC STRENGTHS

APPENDIX A

EFFECTS OF SPECIMEN SIZE ON CERAMIC STRENGTHS

ABSTRACT

Fracture stresses in specimens of four commercial polycrystalline ceramics differing in each linear dimension by a factor of four or five were measured at room temperature under controlled conditions. Data obtained were analyzed with the aid of fractographic examinations for applicability of Weibull statistics.

INTRODUCTION

Brittle fracture is triggered in a ceramic by tension acting at the site of a small discontinuity or flaw which intensifies the stress locally. Fracture occurs according to Griffith's criterion, as follows[1]*:

$$\sigma_f = \frac{K_{IC}}{s} \qquad \text{(A-1)}$$

where σ_f is tensile stress at the flaw site, K_{IC}, is critical stress intensity factor of the material, and s is flaw severity**. If K_{IC} is considered a bulk property and the ceramic to contain a homogeneous population of identical worst flaws, it would be expected to fail at a unique tensile stress. However, strength values of nominally identical specimens when tested alike are usually dispersed because of specimen-to-specimen variability in fracture-initiating flaws. This variability precludes assigning a unique strength value to specimens of a given size and causes a size dependence of strength. Large specimens

* References begin on page A-23.

** $s = Y\sqrt{a}/Z$, where Y and Z are dimensionless parameters and a is flaw depth[2].

tend to fail at lower mean strengths than small ones simply because there is apt to be a more severe flaw among the greater number of flaws in the large specimen. For specimens of the same size, the effective size is smaller when failure is by bending than by direct tension[3], because only part of the specimen is subjected to tension in bending.

A central problem in structural designing with brittle materials results from this size dependence of fracture stress. With a size dependence, strength obviously cannot be described for purposes of structural analyses in terms of stress alone.

The object of the present research was to define and interpret the effects of size on strengths of four commercial polycrystalline ceramics. Emphasis was placed on precision in determining strengths, and fractography was used in interpreting strength-size data.

MATERIALS AND METHODS

A glass-ceramic, a conventionally sintered alumina, a hot-pressed alumina, and a hot-pressed silicon nitride were studied. Physical properties of each material are given in Table A-1. Grain-sizes (G) and densities (ρ) are as reported by the manufacturers. Young's moduli (E) were determined in direct compression from measurements of load as a function of average strain. Critical stress-intensity factors, K_{IC}, were determined by the double-torsion technique[4].

TABLE A-1. MATERIAL PROPERTIES

	G, μm	ρ, g/cm^3	E, GNm^{-2}	K_{IC}, MNm$^{-3/2}$
Glass-Ceramic[a]	1-2	2.60	114	2.38 ± 0.08
Sintered Alumina[b]	5	3.75	318	3.84 ± 0.05
Hot-Pressed Alumina[c]	1-2	3.90	413	4.19 ± 0.15
Hot-Pressed Si_3N_4[d]	1-2	3.20	310	4.24 ± 0.30

(a) Corning's Pyroceram 9606
(b) 3M Co.'s Alsimag 614
(c) AVCO's 99.8% Al_2O_3
(d) Norton's NC-132

Bend-test specimens for strength determinations were cut from billets with a diamond saw, and were finish-ground parallel to the tensile-stress direction with a 320-grit diamond wheel. Edges were rounded slightly by polishing with a 1-μm diamond paste to prevent edge-initiated fractures.

Room-temperature bend tests were conducted on specimens of two sizes of each material. Small specimens of all four materials were 0.1 by 0.2 by 1.5 in. Each linear dimension of the large glass-ceramic and sintered-alumina specimens was five times that of the small specimen; the large hot-pressed alumina and silicon nitride specimens were larger by a factor of four.

Specimens were tested in 3- or 4-point bending using the bend-test fixture designed by Hoagland, et al.[5] Only small specimens were tested in 3-point bending over a span of 1.25 in. In the 4-point bend tests on small specimens, outer and inner spans were 1.25 and 0.75 in., respectively, and on large specimens they were four or five times those on small specimens, corresponding to the ratio of linear dimensions between the large and small specimens.

Strength tests on materials except silicon nitride were conducted under conditions that either restricted or enhanced subcritical crack growth. Specimens were tested in dry nitrogen at a stress rate of 100 MNm^{-2}/sec to restrict subcritical crack growth, and in distilled water at a stress rate of 4 MNm^{-2}/sec to enhance such growth. Specimens of Si_3N_4 were tested in laboratory air (relative humidity 45 percent) at a stress rate of 100 MNm^{-2}/sec.

Strengths, σ, were calculated from the expression, $\sigma = Mc/I$, where M is the applied moment, c is one-half the specimen thickness, and I is the cross-sectional moment of inertia.

After strength testing, the site (whether surface or subsurface) and the type of the fracture-initiating flaw in each specimen were identified by examination of the fracture surface using both optical[6] and scanning-electron microscopy[6,7,8].

RESULTS

Strengths of the glass-ceramic specimens, excluding those which failed from edge-initiated fractures, are given in Table A-2. Strength specimens were cut from three billets (each 1 x 5 x 10 in.). Because of different microstructures specimens for each billet required separate strength analyses. This seriously limited the number of replicate specimens available for statistical treatment of strength data. Strengths of specimens of the other three materials are given on two-parameter Weibull plots (i.e., as log σ versus log log $[1/(1-P)]$, where P is the probability of fracture) in Figures A-1, A-3, and A-4. Results of the fractographic examinations are given in the discussion which follows.

DISCUSSION

Strength of Glass-Ceramic Specimens

As shown in Table A-2, fracture stress of the glass-ceramic was dependent on whether failure initiated at a machine flaw on the tensile surface or at a subsurface pore; higher fracture stress values were associated with surface origins. It will be noted that subsurface origins were observed only infrequently in tests of small specimens in dry nitrogen, and they were not observed in any specimens tested in water. The increased frequency of subsurface pore origins in large specimens tested in dry nitrogen is attributed to a sparse pore population in the material. The absence of subsurface origins in specimens tested in water is, of course, explained by the larger size of surface flaws in this environment coupled with the expected lack of an atmospheric effect on fracture initiation at internal sites.

An important finding is the lack of an observed strength dependence on specimen size among specimens fracturing from surface origins. In these instances, large and small specimens from each

TABLE A-2. BEND STRENGTH OF THE GLASS-CERAMIC

Environment	Specimen Size	Type of Loading	Fracture Origin	No. of Observations	Average Fracture Stress (MNm^{-2})	Coefficient of Variation (%)
				Billet A		
Dry N_2	Small	4-point	Surface	7	308	2.5
			Pore	1	243	
Dry N_2	Large	4-point	Surface	3	317	4.4
			Pore	2	265,245	
				Billet B		
Dry N_2	Small	4-point	Surface	8	395	4.2
			Pore	1	326	
Dry N_2	Large	4-point	Surface	2	378,396	
			Pore	3	296	1.1
			Surface-pore	1	383	
Dry N_2	Small	3-point	Surface	11	383	3.5
				Billet C		
Dry N_2	Small	4-point	Surface	5	317	2.2
Water	Small	4-point	Surface	4	204	1.5
Water	Large	4-point	Surface	4	199	1.0

billet exhibited essentially the same average fracture-stress values and small (<5 percent) coefficients of variation. This finding applies to tests conducted in both water and the dry environment, and to comparable data from 3- and 4-point bend tests.

The strength of water-tested specimens was calculated from the dry-N_2 strength and independently determined slow crack growth parameters in water, as follows:

$$\sigma_f = \left[\frac{2\dot{\sigma}(n+1)}{A(Y/Z)^2(n-2)} \left(\frac{\sigma_{IC}}{K_{IC}} \right)^{n-2} \right]^{1/n+1} \qquad \text{(A-2)}$$

where σ_f and σ_{IC} are strengths in water and dry N_2, respectively, $\dot{\sigma}$ is stress rate, Y and Z are test-geometry and flaw-geometry parameters, respectively, and A and n are slow-crack-growth parameters in the following equation:

$$V = A\, K_I^{\,n} \qquad \text{(A-3)}$$

where V is crack velocity at a stress-intensity factor of magnitude K_I. The double-torsion technique was used to determine A and n in slow-crack-growth experiments. There were found to be 10^{-353} and 56, respectively.

The calculated strength was 210 MNm^{-2} which agrees well with the measured strength of 204 $\pm$ 3. This good agreement indicates that the similar surface flaws participated in fracture of specimens tested both in dry N_2 and water, and K_{IC} of the material is independent of environment.

Conventionally, strength values from surface and subsurface flaw origins are averaged together in assigning a strength value to a given ceramic. For purposes of academic interest, strengths from tests in the dry environment have been calculated in this way. As shown in Table A-3, these values exhibit a size effect due to the greater frequency of pore origins in the large specimens.

TABLE A-3. CONVENTIONAL TREATMENT OF BEND STRENGTH DATA OF THE GLASS CERAMIC

Specimen Size	Average Strength (MNm^{-2})	Coefficient of Variation (%)	No. of Specimens
	Billet A		
Small	299	6.7	8
Large	292	15.4	5
	Billet B		
Small	387	5.6	9
Large	341	15.2	6

Strength of Sintered-Alumina Specimens

Strengths of all specimens, excluding those exhibiting edge fractures, given in Figure A-1 indicate that in each environment the stress for any failure probability within the experimental limits of 0.1 and 0.9 decreased with increasing specimen size. The Weibull plots are reasonably linear, indicating that each set of strength data can be described by an equation of the form[3,9]:

$$P = 1 - \exp\left[-\int_{S \text{ or } V} (\sigma/\sigma_o)^m \, dS \text{ or } dV\right] \qquad (A\text{-}4)$$

where m is Weibull modulus, σ_o is a normalizing constant, and the integral is taken over the volume or surface under tension depending on whether subsurface or surface flaws controlled fracture. The modulus, m, as determined by the slopes of the plots, is constant (i.e., 34) only for specimens of differing size tested in water. The separations between the lines representing data from water tests are such that the three sets of data can be represented by a single two-parameter function with constant values of both σ_o and m. For tests in the dry environment, m decreases with increased specimen size; values are 34, 26, and 11 for the small 3-point, small 4-point, and large 4-point bend specimens, respectively.

The equivalance of Weibull moduli from tests of large and small specimens in water (m = 34) and small specimens in dry N_2 (m = 34 or 26) suggests that fractures in these specimens were a consequence of surface flaws from the same statistical population. This matter was investigated further by calculating, using Equation A-2, the strengths in water from dry-N_2 strengths and independent measurements of crack velocity as a function of stress-intensity factor[8]. Table A-4 shows good agreement between the calculated and measured strengths indicating that the same surface flaws initiated subcritical crack growth of specimens in water and catastrophic fracture of small specimens in dry nitrogen.

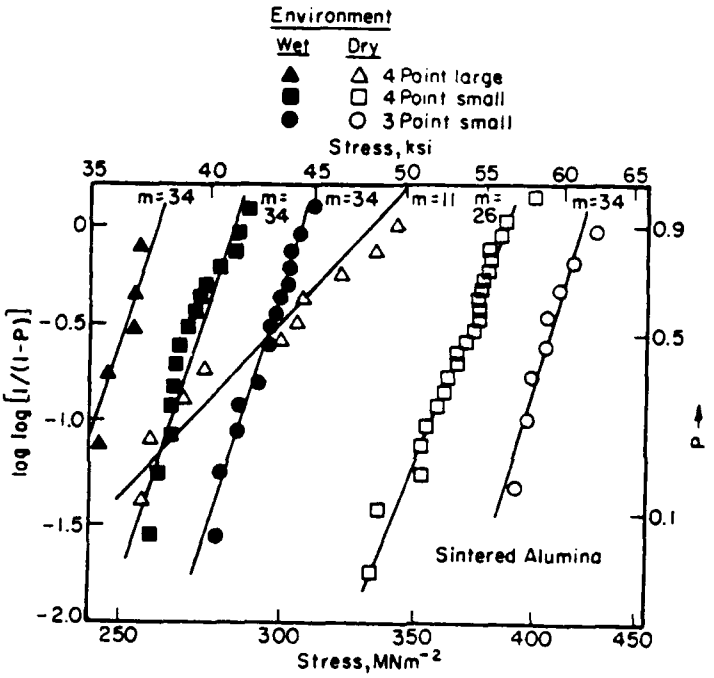

FIGURE A-1. Weibull Plots for Strength-Size Data of Sintered Alumina

TABLE A-4. CALCULATED AND MEASURED STRENGTHS OF SINTERED ALUMINA SPECIMENS IN WATER

Type of Loading	Specimen Size	σ_f, MNm^{-2}		
		Calculated	Measured	
			Avg.	Std. Dev.
3-point bend	Small	288	295	9.4
4-point bend	Small	263	271	9.5
4-point bend	Large	243	250	5.5

Ratios of mean strengths were also calculated using[3]:

$$\bar{\sigma}_1/\bar{\sigma}_2 = (S_2/S_1)^{1/m} \qquad \text{(A-5)}$$

and were compared with experimental ratios (Table A-5).* Equation (A-5) requires constancy of m; the significant differences between m's for data from large and small specimens tested in dry nitrogen precludes similar analysis for tests in the dry environment.

In tests in dry N_2, the larger m exhibited by small specimens (m = 34 or 26) than by large specimens (m = 11) indicates less dispersion in the size of strength-controlling flaws in the small specimens. Fractography supported this indication. The microscopic inhomogeneities at fracture origins in the small specimens ranged from 40 to 70 μm in size whereas those in the large specimens ranged from 150 to 400 μm. The smaller m value for the large specimens also suggests a sparser population of the flaws that initiated fracture in large specimens than of the smaller surface inhomogeneities that initiated fracture in the small specimens. Presumably, if a sufficiently greater number of small specimens had been tested in the dry environment, some would have exhibited "large-flaw" failures. In this event, one would not expect mean strengths of the small specimens to be much different from those reported here, but the low-probability region of the probability-strength curve should be affected significantly. The Weibull plot in this case would be complex (e.g., two straight lines), reflecting a fundamental change in the nature of fracture at some stress level. Figure A-2 demonstrates that is indeed the situation[10]. In Figure A-2, failure probabilities for the small and large 4-point bend data from Figure A-1 have been normalized to those of the small 3-point bend specimen using one of the following Weibull formulations depending on whether volume or surface flaws controlled fracture:

---

* Differences in stress distributions in the 3- and 4-point bend specimens of the same actual sizes made the effective size of the 4-point specimen larger than that of the 3-point specimen by $\approx(3m+5)/5$. This factor was calculated by determining the size of a direct-tension member that has the same P-σ relation as the specimen subjected to nonuniform tension[3]. For the two sizes of 4-point bend specimens, similarity allows use of actual surface-area ratio in Equation (A-5); i.e., $S_2/S_1 = 25$.

TABLE A-5. OBSERVED AND CALCULATED MEAN STRENGTH RATIOS FOR THE SINTERED ALUMINA

Specimens Considered	Environment	Observed	Calculated*
Small 3-point: small 4-point	Water	1.09	1.09
Small 3-point: large 4-point	Water	1.18	1.20
Small 4-point: large 4-point	Water	1.08	1.10
Small 3-point: small 4-point	Dry N_2	1.11	1.09

* Using m = 34.

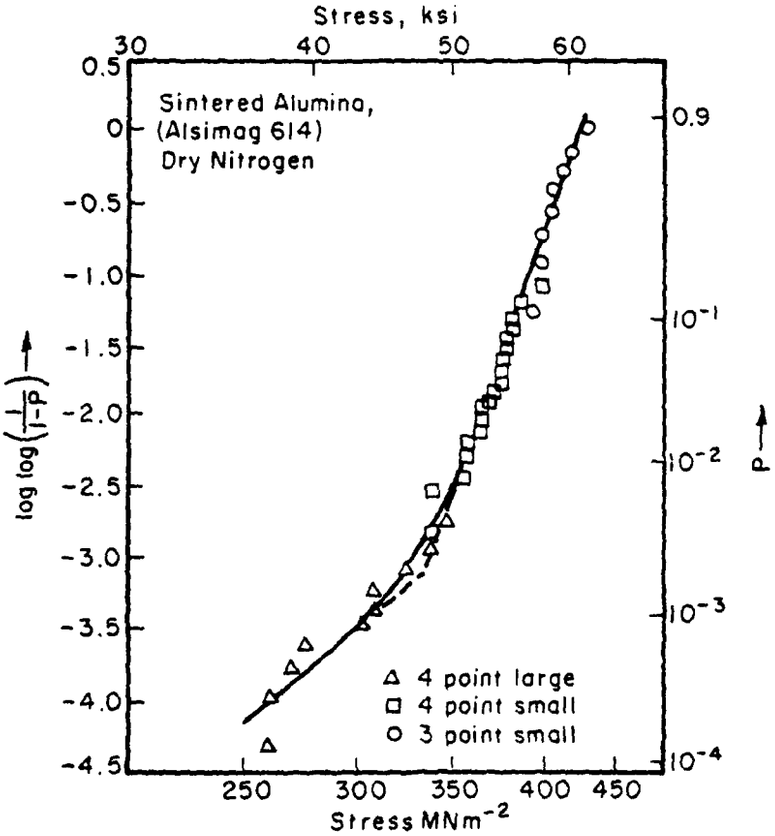

FIGURE A-2. Weibull Plot of the Data Obtained on Three Different Sizes of Sintered Alumina Tested in Dry N_2 (see Fig. A-1) Failure probabilities for the small and large 4-point bend data have been normalized to those of the small 3-point bend specimen (Ref. 10).

$$P_1 = 1 - (1 - P_2)^{V_{E_1}/V_{E_2}} \quad \text{(A-6a)}$$

$$P_1 - 1 - (1 - P_2)^{S_{E_1}/S_{E_2}} \quad \text{(A-6b)}$$

where V_E and S_E are effective volume and surface area of specimens under consideration, and P_1 and P_2 are the failure probabilities of the two sizes of specimens.

Strength of Hot-Pressed Alumina Specimens

The data (Figure A-3) show a qualitative trend of decreasing strength with increasing specimen size in each environment. With an exception of strength data from 3-point bend tests in dry N_2, the Weibull plots do not exhibit the linear relationship required for applicability of Weibull's two-parameter function. Large specimens both in dry N_2 and water failed from several different types of intrinsic flaws in each environment. However, apparent m's for large specimens were similar in the two environments which indicates that similar flaw populations controlled fracture in both environments. The lower strengths in water resulted because subcritical crack growth preceded fracture, and an extended crack linked with an intrinsic flaw.

m for 3-point bend specimens tested both in dry N_2 and water was calculated to be ~17. Although, the fit of the 4-point bend data in dry N_2 to the two-parameter function is poor, similarity of the slope to that of 3-point bend data suggests similar flaw populations controlled fractures in each.

Strength data obtained in water on 4-point small specimens show two distinct regions in Figure A-3. Three different explanations are possible, as follows: (1) two flaw populations controlled fracture, (2) Weibull's 2-parameter function does not apply, and the three-parameter function is more appropriate in describing this set of data, and (3)

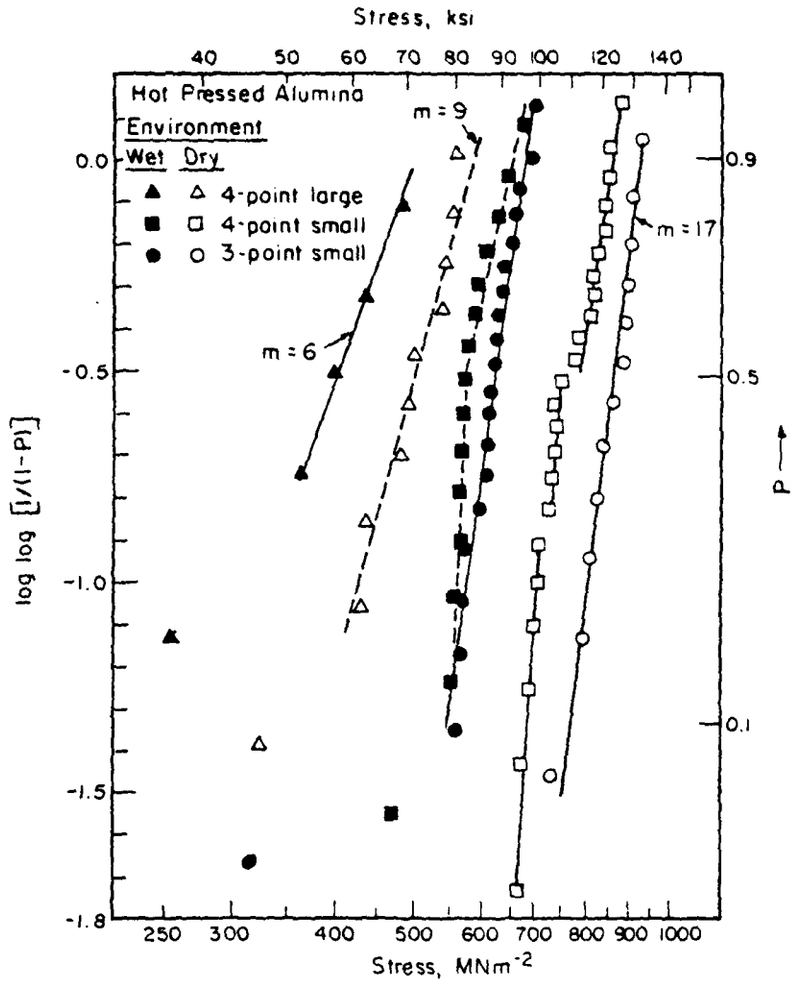

FIGURE A-3. Weibull Plots of Strength-Size Data of Hot-Pressed Alumina

some variable(s) in addition to flaw size is affecting strength. No significant differences were observed in the type of fracture-initiating flaws in these specimens. Also, the parameter, σ_u, which is a measure of stress for zero probability of fracture, should not vary with strength levels and environments[3]. Therefore, the third possibility was explored.

K_{IC} values which controlled strengths of individual specimens were calculated using the following equation[6]:

$$K_{IC} = 0.425\ \sigma_f\ r^{1/2} \qquad \text{(A-7)}$$

where σ_f is the fracture stress at the origin, and r is the radius of the mirror which surrounds the flaw. K_{IC} values so calculated for specimens of different sizes tested in water and dry N_2 are given in Table A-6.

Table A-6 shows no significant differences in the calculated K_{IC} values between large and small specimens tested in dry N_2. Also, tests of large specimens in water gave K_{IC} values similar to those obtained in dry N_2. However, K_{IC} from tests in water on small specimens exhibited higher values and larger dispersions; lower K_{IC} values were generally associated with specimens which failed at higher fracture stresses. Recently, Hübner and Jillek[11] have observed similar effects on K_{IC} of an alumina ceramic. They have attributed the increase in K_{IC} to a microcracked zone forming a three-dimensional network of cracks ahead of a natural crack tip in the presence of moisture-related crack growth. The similarity of K_{IC} values for large specimens tested in water and dry N_2 indicates absence of the microcracked growth in these large specimens, the extended crack invariably linked with an intrinsic hetrogeneity, i.e., large pore, inclusion, or large-grain cluster, which apparently stopped the microcracking in the immediate vicinity of the critical flaw boundary. If K_{IC} varies among individual small specimens tested in water, as indicated,

TABLE A-6. K_{IC} VALUES CALCULATED FROM STRENGTH-TESTED SPECIMENS OF HOT-PRESSED ALUMINA

Specimen Size	Type of Loading	Environment	K_{IC}, $MNm^{-3/2}$
Small	3-point	Dry N_2	4.15 ± 0.20
Small	3-point	Water	4.98 ± 0.38
Small	4-point	Dry N_2	4.35 ± 0.27
Small	4-point	Water	5.40 ± 0.52
Large	4-point	Dry N_2	4.02 ± 0.19
Large	4-point	Water	4.23 ± 0.26

it is surprising that the Weibull modulus for these specimens is nearly the same as that of 3-point bend specimens tested in dry N_2.

Ratios of mean strengths ($\bar{\sigma}$) of small specimens tested in 3- and 4-point bending were calculated using Weibull's surface area formulation [Eq. (A-5)], and m = 17. Table A-7 gives the calculated and observed ratios.

Table A-7 shows a good agreement between the observed and calculated ratio for tests in dry N_2. This indicates that variability in the same flaw population was the primary cause of the size effect on strength. However, the observed and calculated ratios differed by ~10 percent for tests in water; the calculations indicating a larger effect of specimen size than that observed. This can be explained as follows. In both the 3- and 4-point bend specimens, fractures are believed to be initiated from flaws from a single population since fractography revealed no differences in flaw types among individual specimens, and the average size of the flaw prior to subcritical crack growth is larger in 4-point bend specimens on the basis of dry N_2 test results. Because a larger initial flaw size gives a larger crack extension[12], the average critical flaw depth in 4-point bend specimens tested in water is expected to be larger than that in 3-point bend specimens both by virtue of initial distribution of flaw size and of subcritical crack extension. Because K_{IC} increases with the amount of slow crack growth, 4-point bend specimens are, therefore, expected to exhibit higher strengths than those predicted.

Correlation of strengths of the large and small specimens is precluded by the fact that flaws from different populations were responsible for failure in the two cases, both in water and dry N_2[13].

Strength of Silicon Nitride Specimens

Figure A-4 shows a qualitative trend of decreasing strength with increasing specimen size for this material. Data obtained on

TABLE A-7. OBSERVED AND CALCULATED MEAN STRENGTH RATIOS FOR HOT-PRESSED ALUMINA SPECIMENS

Specimens Considered	Environment	Observed	Calculated
Small 3-point: small 4-point	Dry N_2	1.12	1.15
Small 3-point: small 4-point	Water	1.04	1.15

* Using m = 17.

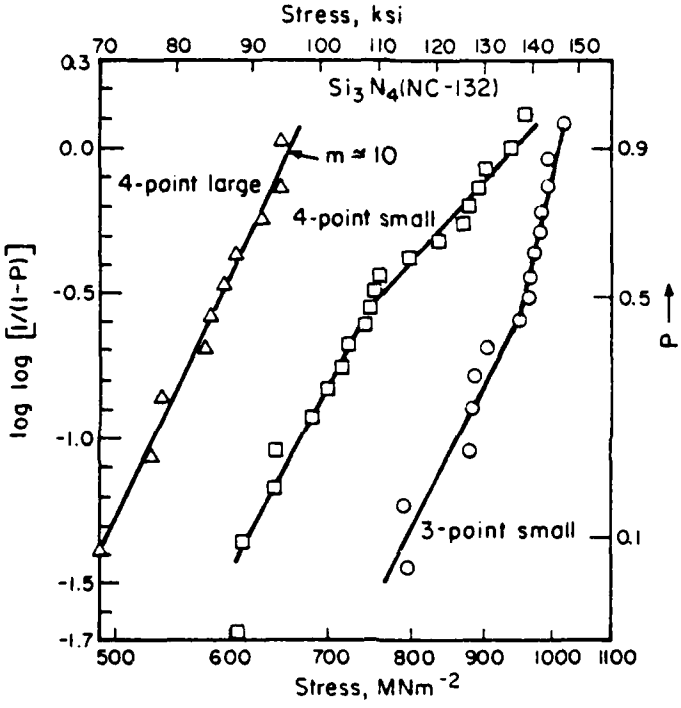

FIGURE A-4. Weibull Plots of Strength-Size Data of Silicon Nitride

large specimens give a reasonable fit to Weibull's two-parameter function, but plots of strength data from small specimens tested in 3- and 4-point bending are not linear. Three different explanations for the nonlinearity, as stated earlier for the case of the hot-pressed alumina, are possible. No significant differences were observed in the type of fracture-initiating flaws in this material. Regardless of specimen size and type of testing, fractures invariably initiated from machining-induced surface flaws[14]. Thus, the explanation based on multi-modal distribution of flaws does not apply. Also, Weibull's three-parameter function can only describe the strength data represented by squares in Figure A-4; it cannot describe the strength data represented by circles[15]. The inability of Weibull's three-parameter function in describing both sets of data tends to preclude its usefulness in explaining the nonlinearity. Therefore, the third possibility of some other variable affecting the strength distribution was explored.

Freiman and coworkers[16] have observed variable critical stress-intensity factors, K_{IC}, associated with individual small specimens of this particular Si_3N_4 material, suggesting that K_{IC} is a local property. We have also found indication of a variation of K_{IC} among individual small specimens, with no consistent trend of variable K_{IC} with strength levels. K_{IC} values calculated from fracture-mirror radii measurements[6] ranged from 2.9 to 5.2 $MNm^{-3/2}$. It should be pointed out that the mirror boundaries were difficult to define precisely; the variability in K_{IC} could be associated with this experimental difficulty and not be real. In this case, some other explanation for the nonlinearity of P-σ data is required.

CONCLUSIONS

Observed size dependencies of strength resulted from specimen-to-specimen variations in "worst" flaws, such that a severe worst flaw was associated with larger effective sizes subjected to tension. Strength, therefore, decreased with increased specimen size. For each ceramic, a single Weibull function was inadequate to describe the strength dispersion over the entire range of observed strength values. This situation resulted in three of the four ceramics studied because more than one population of worst flaws were present in the material, and the population which dominated depended on specimen size, testing environment, and strain rate.

In one of the ceramics, hot-pressed alumina, K_{IC} also varied among specimens. The variation occurred in a consistent manner, increasing with extent of subcritical crack growth. In this case, the effect of variable K_{IC} on strength must be determined independently and strength values adjusted accordingly prior to any statistical treatment of the data to define the size dependence of its strength. In the one ceramic where no evidence was found of more than one population of worst flaws, hot-pressed silicon nitride, the observed strength dispersion for specimens of all sizes studied could not be described clearly by a single Weibull function. The reason was not firmly established, but the existence of a variable K_{IC} in the material is indicated.

Generally, in cases where two worst flaw populations were present, one population was wholly or partially associated with surface finishing and the other with microstructural features. Strength of glass-ceramic specimens surprisingly did not exhibit a size dependence when failure resulted from flaws associated with surface finishing.

REFERENCES

(1) Griffith, A. A., Phil. Trans. R. Soc., A221, 163-198 (1920).

(2) Bansal, G. K., J. Am. Ceram. Soc., 59 [1-2] 87-88 (1976).

(3) Davies, D.G.S., Proc. Br. Ceram. Soc., 22 429-52 (1973).

(4) Williams, D. P. and Evans, A. G., J. Test. Eval., 1 [4] 264-70 (1973).

(5) Hoagland, R. G., Marschall, C. W., and Duckworth, W. H., J. Am. Ceram. Soc., 59 [5-6] 189-92 (1976).

(6) Bansal, G. K., Phil. Mag., 35 [4] 935-44 (1977).

(7) Bansal, G. K., Duckworth, W. H., and Niesz, D. E., Am. Ceram. Soc. Bull., 55 [3] 289-92, 307 (1976).

(8) Bansal, G. K., Duckworth, W. H., and Niesz, D. E., J. Am. Ceram. Soc., 59 [11-12] 472-78 (1976).

(9) Weibull, W., J. Appl. Mech., 18 [3] 293-97 (1951).

(10) Johnson, C. A. and Prochazka, S., Quarterly Progress Report No. 3, prepared for Naval Air Development Center under Contract No. N62269-76-C-0243 (January, 1977).

(11) Hübner, A. and Jillik, W., J. Mat. Sc., 12, 117-25 (1977).

(12) Evans, A. G., Int. J. Fract. Mech., 10 [2] 251-59 (1974).

(13) Bansal, G. K. and Duckworth, W. H., "Strength-Size Relations in a Hot-Pressed Al_2O_3", to be published.

(14) Bansal, G. K. and Duckworth, W. H., "Strength-Size Relations in a Hot-Pressed Si_3N_4", to be published.

(15) Pears, C. D. and Starrett, H. S., Technical Report No. AFML-TR-66-228 (March, 1967).

(16) Freiman, S. W., Mecholsky, J. J., and Rice, R. W., U. S. Naval Research Laboratory, Private Communication (1977).

APPENDIX B

STRUCTURAL DESIGNING WITH CERAMIC MATERIALS

APPENDIX B

STRUCTURAL DESIGNING WITH CERAMIC MATERIALS

ABSTRACT

A central problem in attempting to use ceramic materials in demanding structural applications is uncertainty about the stresses to which they can be safely subjected. A ceramic rarely, if ever, exhibits a characteristic failure stress. This stress depends on the nature and distribution of microscopic flaws that intensify stress locally, and fracture initiates at a single "worst" flaw when Griffith's criterion for crack instability is met. Within the basic framework, theories are available for treating effects of time, size, and stress distribution on failure stress. This paper reviews these theories, and discusses their use in specifying limiting stresses in designing structural members.

INTRODUCTION

Situations are becoming more common where the worth of an engineering concept depends on the assured integrity of a ceramic structural member. These situations usually impose the problem of predicting whether loading conditions will trigger brittle fracture, an event that is characterized by spontaneous crack propagation with little or no prior yielding of the material. Complete loss of the member's structural integrity of course accompanies the event.

This paper intends to provide guidance for structural designers faced with the problem predicting fracture of ceramic components.

GRIFFITH'S FAILURE CRITERION

Brittle fracture is triggered in a ceramic by tension acting at the site of a small discontinuity or flaw which intensifies the stress

locally[1]*. The flaw might be an intrinsic feature of the ceramic's microstructure--a pore, a weak grain boundary, an inclusion, a crack, or a large grain--or it might be an extrinsic scratch, pit, or crack introduced in surface finishing or by abuse in handling or as a consequence of service. In some cases, two or more neighboring flaws of the same or differing kind combine to trigger the fracture event. The photomicrographs in Figure B-1 of fracture-initiating sites exemplify different flaws that were responsible for failure of high-strength ceramic materials.

If the discontinuity is not itself a crack, a crack developes prior to fracture. This crack propagates rapidly and spontaneously when Griffith's criterion for crack instability is met. The criterion can be expressed as follows:

$$\sigma_f = K_{IC}/s \qquad \text{(B-1)}$$

where σ_f is tensile stress, K_{IC} is a proportionality constant, and s is crack severity.

Because brittle fracture is the consequence of a local condition as defined by Equation (B-1), structural designing with ceramic materials imposes a stringent demand for determining tensile stresses that will be experienced at all sites in the component. Local stresses, for example, at sites of load transfer or changes in section, are potentially dangerous and cannot be neglected in the stress analysis. Similarly, in testing ceramic materials to determine fracture stress, it is particularly important to insure that spurious tensile stresses, such as those due to bending in direct tension tests or to wedging or friction in bend tests, do not influence the data. Further, in view of the basic cause of brittle fracture, knowledge of the severity of cracks that pre-exist or might form during service becomes extremely important in considering any specific ceramic material for structural use.

Crack severity, s, in the Griffith relation is determined by the size, shape, orientation, and location of the crack that becomes unstable. It can be defined as follows[2]:

* References begin on page B-27.

$$s = Y \sqrt{a/Z}. \qquad \text{(B-2)}$$

In this equation, a is the depth, in a plane normal to the tensile stress of a surface crack, or in the case of a circular or elliptical subsurface crack, a is, respectively, the radius or half the minor axis. Parameters Y and Z are dimensionless. Normally, Y will depend only on whether the crack extends from a surface, in which case Y = 2.0[3], or is beneath the surface, in which case Y = 1.77. The parameter Z varies with crack shape, having a value of 1.0 for a long shallow crack and increasing with the increasing crack depth-to-width ratio. For a circular crack $Z = \pi/2$[2].

Cracks that become unstable are often called "Griffith" cracks. In ceramic materials they tend to be very small, thwarting attempts to detect them nondestructively. The surface crack responsible for failure in Figure B-1(a) for example was only 8 μm deep*. It should be noted also that the size of a microstructural feature at which fracture might initiate provides only a rough indication of the Griffith crack size as evidenced by a 150-μm-diameter Griffith crack associated with the 70-μm-diameter pore in Figure B-1(b).

The proportionality constant, K_{IC}, in the Griffith relation is known as the material's fracture toughness or critical stress-intensity factor. Ideally, it is considered to be a material constant varying only with temperature, and related to two separate materials properties, Young's modulus (E) and fracture surface energy (γ_f), as follows:

$$K_{IC} = \sqrt{2\gamma_f E} \quad . \qquad \text{(B-3)}$$

K_{IC} is a more fundamental property of a ceramic material than failure stress, σ_f, the value commonly reported for strength. Depending on crack severity, σ_f can vary widely for a given ceramic without K_{IC} being affected. If the severity of the most severe crack in a ceramic component can be specified with certainty, knowledge of K_{IC} permits defining the stress that the component can withstand.

---

* 1 μm = 10^{-4} cm.

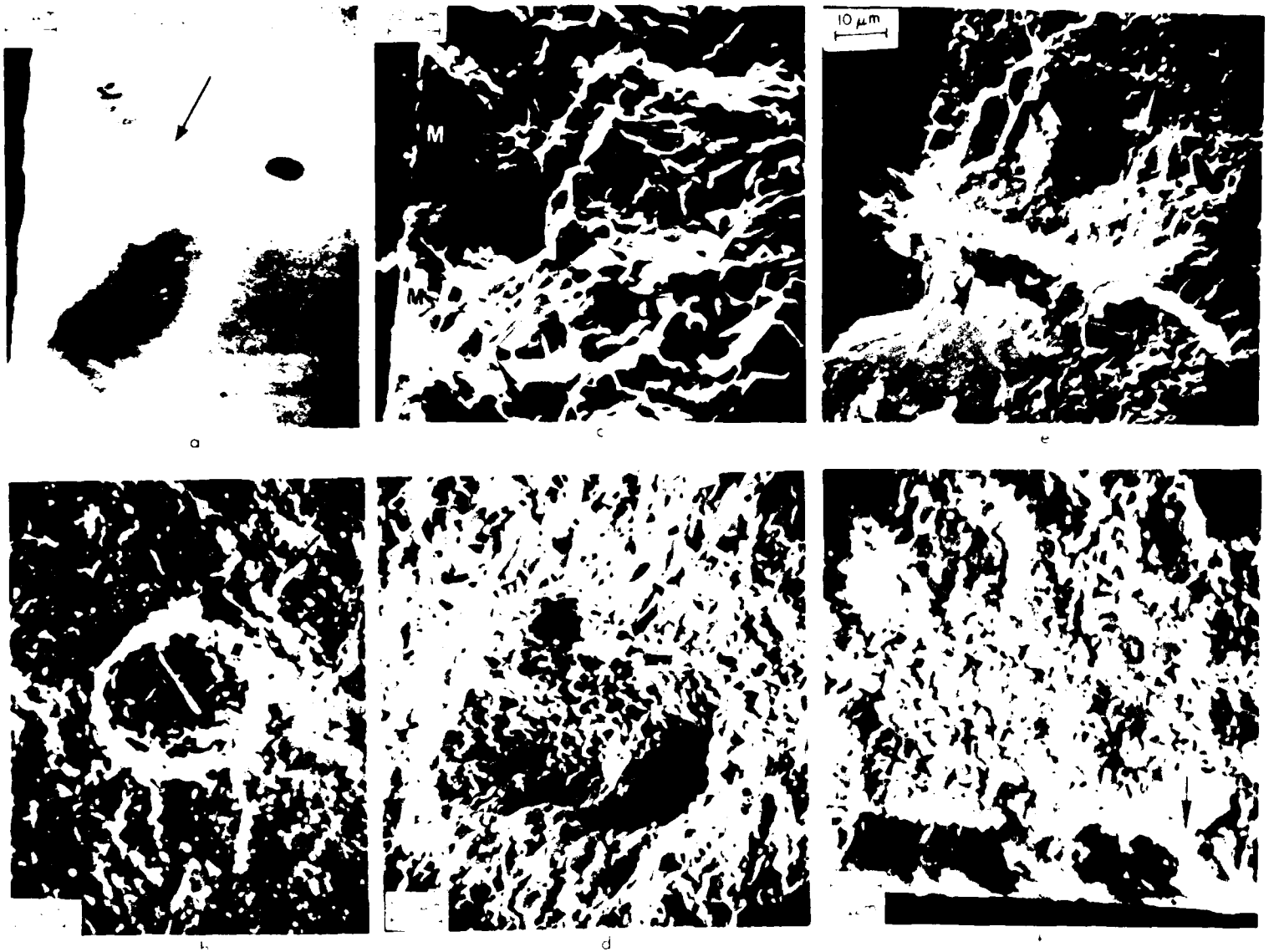

FIGURE B-1. FRACTURE-INITIATING FLAWS IN A GLASS (a), A GLASS-CERAMIC (b) A SINTERED ALUMINA (c) AND (d), A HOT-PRESSED ALUMINA (e), AND A HOT-PRESSED SILICON NITRIDE (f) SPECIMENS. IN (a) AND (f), EXTRINSIC SURFACE FLAWS ~5 TO 10 μm DEEP AND APPARENTLY INTRODUCED DURING MACHINING OF SPECIMENS CAUSED FAILURES. IN (b), (d), AND (e), FAILURES WERE CAUSED BY INTRINSIC FLAWS, A LARGE PORE, A LARGE (~250 μm DIA.) INCLUSION, AND A LARGE-GRAIN AGGLOMERATE, RESPECTIVELY. IN (c), A SMALL INTRINSIC FLAW, I.E., A 40μm LONG PORE, LINKED WITH TWO EXTRINSIC MACHINING FLAWS AT M ON THE TENSILE SURFACE PRIOR TO FRACTURE

Table B-1 gives experimentally-determined room-temperature values of K_{IC} for several ceramics[4-9]. A word of caution is in order about accepting such values as material constants. In some ceramics, K_{IC} is found to vary because of variations in local conditions at the site of the Griffith crack with which it is associated[5-8].

TIME AND SIZE DEPENDENCIES OF CERAMIC STRENGTHS

Ceramic materials often exhibit so-called "static fatigue"[10]. Fracture is delayed, occurring after a stress has been sustained for some period of time. Coincident with static fatigue, strengths increase with increasing stress or strain rates. Also, ceramic strengths usually decrease with increasing specimen size.

Both of these phenomena, the time and size dependencies of strength, must be considered in any attempt to assure safe loading conditions for a ceramic component subjected to tension, and both have been interpreted in a manner consistent with the Griffith criterion for brittle fracture.

Effect of Time

The time dependency of fracture stress is a consequence of a slow, stable growth which increases the severity of existing cracks. It occurs in a reactive environment or at high temperatures where the ceramic exhibits creep. In the case of silicate glasses and most oxide ceramics, the presence of moisture causes the environment to be reactive, even at room temperature[10]. Under the combined influence of a reactive environment and tension, a crack will grow slowly until the Griffith criterion for crack instability is satisfied, and spontaneous, very rapid growth ensues. The crack might change shape during stable growth, and this in addition to the growth alters its severity [see Equation (B-2)].

TABLE B-1. ROOM TEMPERATURE K_{IC} VALUES FOR SEVERAL CERAMICS

Material	K_{IC}, $MNm^{-3/2}$
Soda-Lime Glass[4]	0.75 ± 0.03
Glass-Ceramic (9606)[4]	2.38 ± 0.08
Sintered Alumina (Alsimag 614)[4]	3.84 ± 0.05
Hot-Pressed Alumina[4,5,6]	4.2 - 5.8
Hot-Pressed Si_3N_4 (NC-132)[7,8]	4.0 - 6.0
Sintered SiC[9]	4.0

The velocity, V, of subcritical crack growth in a given ambient has been found related to stress-intensity factor, K_I, as follows[11]:

$$V = A K_I^n \tag{B-4}$$

where A and n are empirical constants for a given temperature and environment.

With knowledge of A and n, the time at which fracture will occur can be calculated. Assuming no change in crack shape (i.e., in Z) or K_{IC} during growth, the time to failure, t, under a constant tensile stress, σ, is as follows[10,11]:

$$t = \frac{2Z^2}{AY^2(n-2)} \left(\frac{K_{IC}}{\sigma_{IC}}\right)^{2-n} \sigma^{-n} \tag{B-5}$$

where σ_{IC} is fracture stress in an inert environment (i.e., in the absence of slow crack growth). Similarly, one can calculate the effect of stress rate or strain rate on strength. The relation between stress rate, $\dot{\sigma}$, and strength is as follows[11]:

$$\sigma_f = \left[\frac{2\dot{\sigma}(n+1)}{A(Y/Z)^2(n-2)} \left(\frac{\sigma_{IC}}{K_{IC}}\right)^{(n-2)}\right]^{1/(n+1)} \tag{B-6}$$

where $(\sigma_{IC}-\sigma_f)$ is the strength degradation due to subcritical crack growth. Since ceramic materials rarely deviate much, if at all, from linear elastic behavior, strain rate, $\dot{\varepsilon}$, is proportional to stress rate; i.e., $\dot{\varepsilon} = \dot{\sigma}/E$, where E is Young's modulus.

Table B-2 gives strength values for ceramic specimens tested in water and in dry nitrogen. Subcritical crack growth occurred during testing with a constant stress rate of 4 MNm^{-2}/sec in water, and was absent during testing in dry nitrogen at a stress rate of 100 MNm^{-2}/sec. Table B-2 also includes calculated strengths in water given by Equation (B-6). Values for A and n used in the calculation were determined from independent slow crack growth experiments in water[12].

TABLE B-2. CERAMIC STRENGTHS IN DRY NITROGEN AND WATER

Ceramic	Type of Loading	Average Strength, MNm^{-2}		
		Dry Nitrogen	Water	
			Measured	Calculated*
Sintered Al_2O_3	3-point bending	408	295	288
Sintered Al_2O_3	4-point bending	369	271	263
Glass-Ceramic	4-point bending	317	204	210

* Calculated from dry-nitrogen strengths with Equation (B-6). Values of A and n used in the calculation were determined in slow-crack growth experiments as 10^{-276} and 42, respectively, for the sintered Al_2O_3 and 10^{-353} and 56 for the glass-ceramic.(12)

It is significant to note from the data in Table B-2 that the subcritical crack growth in water reduced the strength of the glass-ceramic by one-third and of the alumina ceramic by one-fourth. Some ceramics (e.g., silicon nitride) would have suffered little or no strength degradation in water, and others no doubt would have suffered more. Surface flaws were responsible for failure of both ceramic materials in dry nitrogen as well as in water. Had subsurface flaws caused failures in dry nitrogen, we would not have obtained the excellent correlation between calculated and measured strengths in water. Equations (B-5) and (B-6) require that the surface flaws that exhibit subcritical crack growth be responsible for failure in the absence of such growth. Also, as indicated above, the equations require that K_{IC} be a material constant, unaffected by test environment or local conditions at the crack-initiation site, and that Z, the crack-shape parameter, not changed much during the subcritical growth.

Clearly, if the surface of a ceramic structural component is to be subjected to significant tensile stress, the designer must determine whether the material's strength degrades in the service environment and, if it does, account for subcritical crack growth in establishing safe loads. It is also apparent that careful attention must be given to the environment and stress rate as well as the temperature in obtaining strength data for use in designing a component. Further, the selection of a ceramic for a component should not be based solely on strength, but on the subcritical crack growth rate as well.

Effect of Size

The Griffith relation tells us that fracture occurs when the stress-intensity factor, K_I, the product of tensile stress, σ_t, and crack severity, s, reaches a critical level, K_{IC}, at any site in a ceramic. It follows that the level of K_I throughout a component determines whether it will withstand intended loads. A stress analysis of course

provides the needed knowledge of the σ_t distribution in the component, but knowledge of s cannot be readily obtained.

As indicated previously, s depends on the size, shape, and location of a single flaw in the ceramic. If the ceramic contained a homogeneous population of identical "worst" flaws, it would be expected to fail at a unique tensile stress. In this case, a value of critical stress could be predetermined from strength tests and used as the failure criterion in structural designing. However, we normally observe that strength values of nominally identical specimens when tested alike are dispersed, and the values for individual specimens are in general inversely related to the size of flaws found microscopically at fracture origins.

Recognition that variability in worst flaws precludes assigning a unique strength value to a ceramic is of paramount importance in structural designing. One consequence of the variability in worst flaws is a size dependence of strength. Large specimens tend to fail at lower mean strengths than small ones simply because there is apt to be a more severe flaw among the greater number of flaws in the large specimen. For specimens of the same size, the effective size is smaller when failure is by bending than by direct tension[13], simply because only part of the specimen is subjected to tension in bending and, even then, the tension gradient tends to cause low values of K_I in regions near the neutral axis.

Two approaches are available to the designer for finding out whether K_I achieves the critical level, K_{IC}, at any site in a component. The most positive is preservice proof testing[14]. In this approach, the component is subjected to a loading that imposes the maximum tensile stresses throughout that will be encountered in service. If the component survives the test, it is placed in service. Due account must be taken for any subcritical crack growth that might occur in service (and in the proof testing itself) when this approach is used. We have discussed treatment of the effect of subcritical crack growth on fracture stress in the preceding section. Also, proof testing requires that

the component surface be representative of that which develops in service. Proof testing of a component with a finished surface would be meaningless if surface flaws are responsible for fracture either in proof testing or service and the finish is lost from service-incurred chemical attack or physical abuse.

Proof testing appropriately conducted assures the integrity of a ceramic structural member, and should be employed in qualifying the member. However, if used as the primary design tool its cut-and-try nature obviously is not well suited for analytically predicting performance or for optimizing a design, and if the component is large or has a complex shape, the cost and time involved in fabrication to arrive at a satisfactory design through proof testing could be prohibitive.

The other available approach is analytical and less positive than proof testing. It is the statistical approach, based on laws of probability. Statistical theories of fracture strength, of which Weibull's is most prominent, treat the scatter among individual strength values caused by variations in the severity of worst flaws in a way to provide a mathematical basis for predicting failure from laboratory strength data for any size component with any tensile-stress distribution in it.

Application of Weibull Statistics[15]

The statistical theories of fracture strength attach special significance to the dispersion of ceramic strength values. They treat the dispersion as an inherent property of the ceramic, reflecting effects from an assumed identical distribution of numerous flaws in any piece of the material. The theories usually assume that fracture of individual specimens occurs in accordance with the Griffith criterion; i.e., when K_I reaches a critical level at some site in the specimen.

Because they describe a ceramic's strength by formulations that contain parameters obtained empirically from the dispersion of strength values, the use of statistical theories as a design tool requires that much care be exercised to insure applicability of strength data. Precautions to be taken include the following:

- Data Quality. If the dispersion reflects testing errors in assessing strengths of individual specimens, the dispersion obviously is not an inherent property of the material and should not be used for characterizing strength.
- Nonrepresentative Data. If the processing of strength specimens differs from that of the component in a way that affects the population density or severity of strength-initiating flaws, the use of the strength data obviously would be misleading. In this connection, flaws introduced at corners during grinding and surface finishing often are responsible for failure in ceramic strength specimens. These edge failures constitute a major cause of nonrepresentative data.
- K_{IC} Variability. Since strength of an individual specimen depends on K_{IC} as well as flaw severity, K_{IC} must be invariant or vary randomly. Otherwise, K_{IC} variations will bias strength dispersions.
- Flaw Location. There must be assurance that the flaws responsible for failure of both the strength specimens and the component have the same location. If surface flaws are responsible for failure in one case and subsurface flaws in the other, a description of strength obtained from the specimens will not describe the component's strength. As will be shown later, failures in the same ceramic can result both from extrinsic surface flaws associated with the surface finish and

from intrinsic subsurface flaws associated with microstructural features. For ceramics exhibiting such bimodal failures, no single statistical formulation can describe the ceramic's strength.

- Service Effects on Extrinsic Flaws. If surface flaws associated with finishing are responsible for failure of strength specimens, the strength data can only be used if these flaws remain unchanged during service exposure and continue to be responsible for failure.

Treatment of Ceramic Strength Dispersions

To mathematically describe strength in the statistical approach the probability of failure, P, as a function of stress, σ, is determined from the dispersion of values in a set of strength data*. Individual values are ordered from weakest to strongest, and each is assigned a probability of failure based on its ranking, n, as follows:

$$P = \frac{n}{N+1} \tag{B-7}$$

where N is the total number of data points.

Examples of P-σ plots from well-controlled strength tests of ceramic materials are shown in Figure B-2. Failure probabilities in any such plot will always be less than one and greater than zero. Equation (B-7) shows that the probability range is determined solely by the number of data points. If 20 specimens are tested P will range from 0.0476 to 0.9524, and if 100 specimens are tested the range is extended from 0.0099 to 0.9901. The probability range covered by the available data is very important in the statistical approach because the design stress is based on an acceptable failure probability. For example, if failure of one component in 100 is tolerable, the stress corresponding

* The maximum tensile stress in the specimen at failure is used. If stress is nonuniform, as in bending, the statistical formulation takes this into account. In contrast, the Griffith relation [Equation (B-1)] requires the actual tensile stress at the site of fracture initiation.

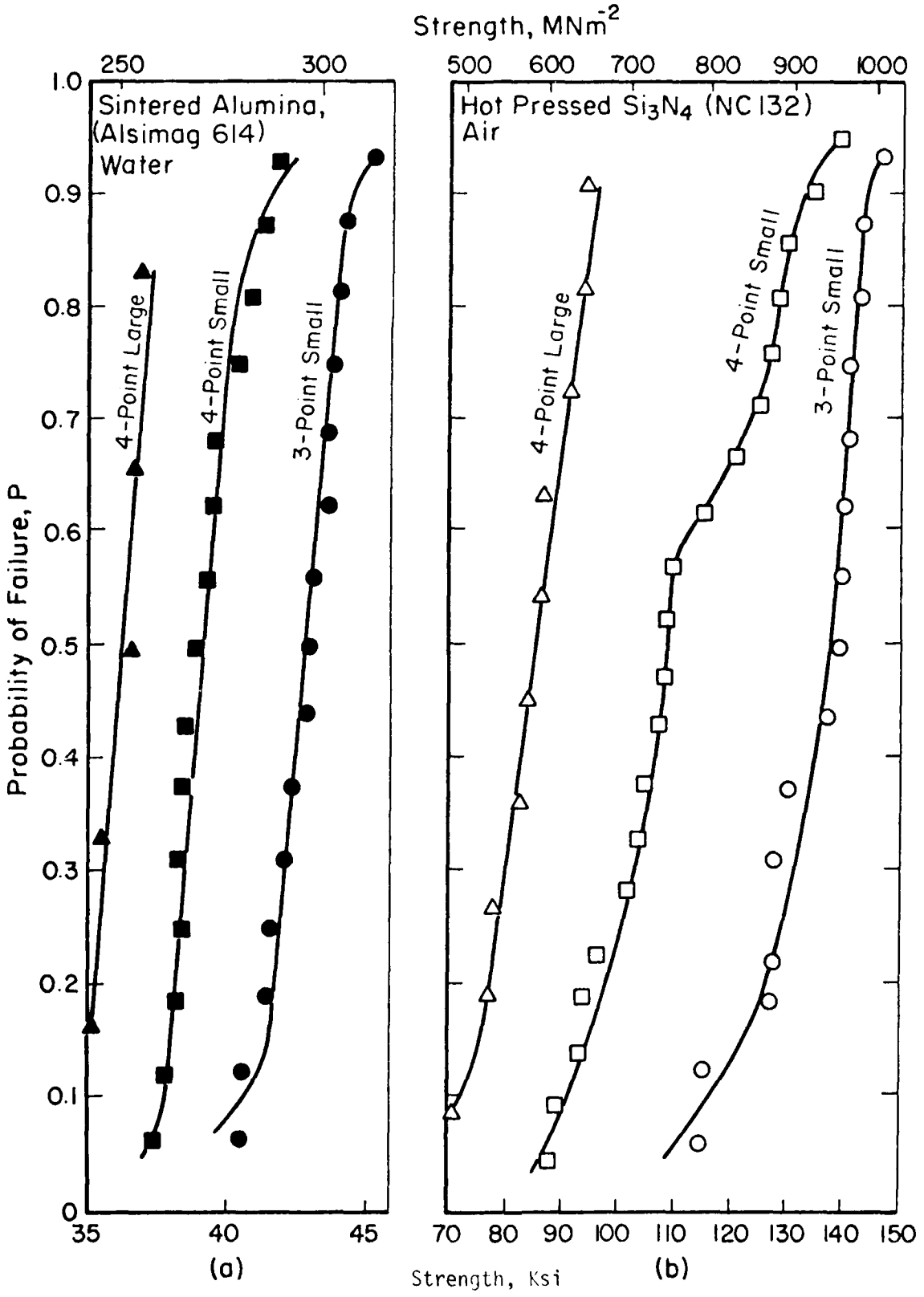

FIGURE B-2. Strength-failure probability curves from room-temperature bend tests of two polycrystalline ceramics. The small specimens of both ceramics were 0.1 x 0.2 x 1.5 in. The large specimens of the alumina ceramic were 0.5 x 1.0 x 7.5 in., and those of the silicon nitride were 0.4 x 0.8 x 6.0 in.

to an 0.01 probability for the component size and stress distribution is chosen for the design stress. Since no basis exists for extrapolating P-σ curves, an adequate number of data points must be obtained so that the acceptable failure probability is within the range of experimentally determined failure stresses.

Weibull's formulation offers a mathematical description of effects of size and stress distribution on P-σ curves for a material[13,15]. In principle, the mathematical description requires only an empirical P-σ curve for a specimen of known size fractured in a test which imposes a defined tensile stress distribution. Weibull's basic expression for the failure probability of a material is as follows:

$$P = 1 - \exp\left[-\int_V (\sigma/\sigma_o)^m \, dV\right] . \qquad \text{(B-8)}$$

The integral is taken over all volume elements, dV, subjected to tensile stress; σ is the maximum tensile stress in the stress field; m, the Weibull modulus, is a measure of the variability of failure stress. Large values of m (e.g., greater than about 30) reflect little scatter and a small effect of size on the material's strength. σ_o is a normalizing constant.

The above form of the Weibull function applies to failure from subsurface (volume) flaws. If surface flaws are responsible for failure of the material, the function should be integrated over the surface subjected to tensile stress rather than the volume; i.e., dV is replaced with dS. Another variation can include a third material constant, σ_u, for materials that exhibit a finite stress for zero probability of failure. The two-parameter form of Equation (B-8) is for the case of zero probability of failure when no tensile stress is present. The three-parameter form uses the quantity $(\sigma-\sigma_u)$ in place of σ in Equation (B-8).

Equation (B-8) can be manipulated and rearranged to yield:

$$\log \log \left[\frac{1}{1-P}\right] = \log \sigma + \log \frac{V \log e}{\sigma_o^m} . \qquad \text{(B-9)}$$

This is an equation of a straight line that allows convenient graphical representation of data. Its utility is illustrated by consideration of Figure B-3 giving plots of $\log \log \left\{\frac{1}{1-P}\right\}$ versus $\log \sigma$ (Weibull plots)

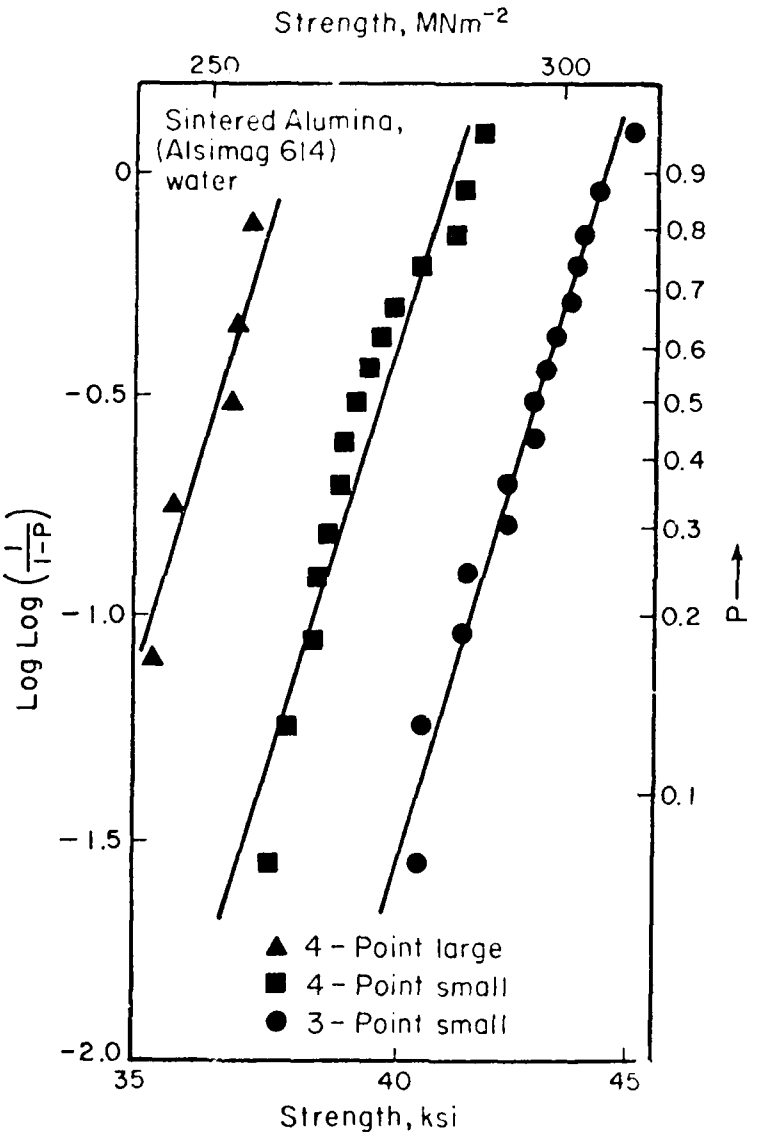

FIGURE B-3

FIGURE B-3. Weibull plots of strength-size data reported in Fig. B-2 (a).

for data presented in Figure B-2(a). The Weibull plots are three parallel straight lines. A straight line is obtained when the strength dispersion can be described by Weibull's two-parameter function; m is the slope of the line. The fact that the three sets of data, representing specimens of different size or subjected to different loading geometries, give parallel straight lines means that a single two-parameter function describes the entire range of observed failure stresses provided that the lines have the proper separations.

The intercept of any of the three lines permits evaluation of σ_o. In the case of this particular ceramic, surface flaws were responsible for fracture, so the appropriate form of the Weibull function contains S rather than V, and from Equation (B-9) the intercept provides the value of $\log \left\{ \frac{S \log e}{\sigma_o^m} \right\}$ from which σ_o can be extracted.

With knowledge of m and σ_o and assurance of the applicability of Weibull's two-parameter function, Equation (B-8) can be used to define the P-σ relation for the σ range covered by the experimental data, regardless of component size, shape, or loading configuration. With this powerful tool the designer can calculate the tensile stress that he can permit in a component with assurance of an acceptable failure probability.

The integration of Equation (B-8) has been treated comprehensively by Weibull[15] and others[13], particularly from the standpoint of obtaining the P-σ relation for a component from an experimentally determined P-σ relation when the tensile-stress distribution in the component differs from that in the test specimen; e.g., use of bend-test data to obtain failure probabilities for a component subjected to uniform tension. This problem is handled mathematically by determining the size of a direct-tension member that has the same P-σ relation as the specimen or component subjected to nonuniform stress. Then, rather than using the actual volume or surface area in Equation (B-8), the uniform-tension equivalent or effective size is used[13]. The effective size (V_E or S_E) of a simply supported centrally loaded square beam for example is $\frac{V}{2(m+1)^2}$ or $\frac{S}{4(m+1)^2}$, where V and S are the volume and surface area, respectively, of material in the span between supports[13].

The following general relation is of key importance in structural designing with ceramics whose strengths can be described by a Weibull formulation[16]:

$$P_1 = 1 - (1 - P_2)^{V_{E_1}/V_{E_2}} \qquad \text{(B-10a)}$$

or in the case of failure from surface flaws:

$$P_1 = 1 - (1 - P_2)^{S_{E_1}/S_{E_2}} \quad . \qquad \text{(B-10b)}$$

Equation (B-10) gives the relation between failure probabilities, P_1 and P_2, at a given stress for two members having different effective sizes. By treating effective sizes the equation is independent of stress distribution in either member. To illustrate use of the equation, suppose a component is to be designed on the basis of data in Figure B-3, a 5 percent probability of failure is acceptable, and the component has an effective surface area 1/10 that of the specimen represented by closed triangles. Substituting in Equation (B-10b):

$$0.05 = 1 - (1 - P_2)^{1/10}$$

so $P_2 = 0.4$ for the specimen, and the stress corresponding to this failure probability from the plot in Figure B-3 is 245 MNm^{-2}. This then is the maximum allowable tensile stress in the hypothetical component.

Equation (B-11), below, is a corollary to Equation (B-10). It is the relation between stresses for a given failure probability of two members having different effective sizes.

$$\sigma_{f_1}/\sigma_{f_2} = (V_{E_2}/V_{E_1})^{1/m} \qquad \text{(B-11a)}$$

or

$$\sigma_{f_1}/\sigma_{f_2} = (S_{E_2}/S_{E_1})^{1/m} \quad . \qquad \text{(B-11b)}$$

Equation (B-11) is frequently used to predict the mean strength (0.5 failure probability) of a member from strength data obtained in tests of specimens of a different effective size.

Since Equations (B-10) and (B-11) are limited in applicability to the range of failure stresses observed in strength tests, they tend to dictate the effective size of specimen(s) that should be strength tested. If the specimen has a significantly smaller effective size than the component, one can expect to have to test a very large number of specimens in order to define the P-σ relation covering the failure stress range of interest, but the range can be encompassed with relatively few data points if the effective size of the specimen is nearly equal to or larger than the component.

Significance of Weibull Modulus

Strength values for ceramic materials are normally reported as the mean failure stress of a series of specimens. The mean value in the statistical approach is the 0.5 failure probability level, a level that will rarely be used as the basis for a design. It signifies that half the components can be expected to fail. If the acceptance failure probability is less than 0.5, the allowable stress must be less than the mean by an amount depending on the material's Weibull modulus, m. Further, if the effective size of the component is larger than that of the specimen, this too will reduce the allowable stress, regardless of acceptable failure probability, to an extent also dependent on the material's Weibull modulus.

Table B-3 shows these reductions in allowable stress for two hypothetical ceramic materials that fail from volume flaws and exhibit the same reported strength of 50,000 psi. One ceramic has a Weibull modulus of 8, and the other has a modulus of 32. It can be seen from the table that for a failure probability of 0.01, the allowable stress is reduced to 29,400 and 43,800 psi, respectively, for materials with Weibull moduli of 8 and 32 if the component's effective size is the same as that of the specimen. When the component's effective size is 1,000 times that of the specimen, these allowable stresses become 12,400 and 35,300 psi.

TABLE B-3. EFFECT OF EFFECTIVE SIZE AND WEIBULL MODULUS ON ALLOWABLE STRESS

Failure Probability	Allowable Stress, 10^3 psi			
	V_E	$10V_E$	10^2V_E	10^3V_E
		m = 8		
0.5*	50.0	37.5	28.1	21.1
0.05	36.4	27.0	20.3	15.2
0.01	29.4	22.0	16.5	12.4
		m = 32		
0.5*	50.0	46.5	43.3	40.3
0.05	46.1	42.9	39.9	37.1
0.01	43.8	40.8	37.9	35.3

* Probability corresponding to mean failure stress; the normally reported strength.

From this example, it is quite clear that the best ceramic for a given structural application will not necessarily be one with the highest mean failure stress (strength) in a standardized test, but will be one that combines high strength with a high Weibull modulus. Both of these properties are subject to upgrading by processing refinements and often by surface-finishing refinements. The prospects for such refinements should not be overlooked in considering a ceramic for structural use.

Complex Strength Dispersions

So far we have discussed primarily ceramics whose strength dispersions can be described by a single Weibull's two-parameter function. Although adequate data on a large number of ceramics are unavailable for a broad generalization, there are indications that applicability of a single two-parameter function is more an exception than the rule.

The simplest complication to be expected is the case where Weibull's three-parameter function applies. In this case, a two-parameter Weibull plot such as in Figure B-3 will yield a curved line bending downward rather than a straight line. To obtain a mathematical description of strength in this case, $\log \sigma$ is replaced by $\log (\sigma-\sigma_u)$ as the plot's abscissa, and σ_u adjusted to a value that yields a straight line. Then, rather than Equation (B-8), Weibull's basic equation for the material's failure probability becomes:

$$P = 1 - \exp - \int_V \left\{ \frac{\sigma-\sigma_u}{\sigma_o} \right\}^m dV \quad . \tag{B-12}$$

This constitutes a rather modest variation of the two-parameter mathematical description of strength*.

* If members are proof-tested, the proof-test stress becomes the stress for zero failure probability, σ_u, for the surviving members.

A more common complication encountered in strength analysis of ceramic materials is the presence of more than one worst flaw population in the material. In this case, the two-parameter Weibull plot will tend to be a curved line bending upward. If the curve can be represented clearly by two or more two- or three-parameter plots, strength can be described in terms of separate Weibull functions for different failure-stress ranges. The intersection of the straight lines gives the failure stress at which control of failure shifts from one type of flaw to another.

A good example of such bimodal failure is provided by the radically different flaws shown in Figures B-1(c) and B-1(d) which were responsible for failure of two specimens of the same ceramic. The small surface flaws shown in Figure B-1(c) controlled failure at high stresses, and the P-σ relation in their stress range could be described by a two-parameter Weibull functions with $m \simeq 30$. At low failure stresses the large subsurface flaws shown in Figure B-1(d) controlled failure, and the P-σ relation for their stress range also could be described by a two-parameter Weibull function, but with $m \simeq 11$. For this ceramic, there was a tendency for strength data from small specimens to be dominated by failures from the small surface flaws and data from large specimens to be dominated by failures from the large subsurface flaws[17]. Figure B-4 is a single two-parameter Weibull plot of strength data for the ceramic obtained from tests of specimens having three different effective sizes. P-σ data from two of the sizes have been adjusted using Equation (B-10) to the effective size of the third specimen[16,17].

Another complication that has been encountered in strength analyses of ceramics is caused by variations of K_{IC}. If K_{IC} varies randomly, its effect on the P-σ relation can become simply all or part of the statistical variation treated by a Weibull function. However, if K_{IC} is a function of failure stress (or flaw severity), its effect must be determined independently and accounted for through an adjustment of strength values for a Weibull plot. Specimen-to-specimen

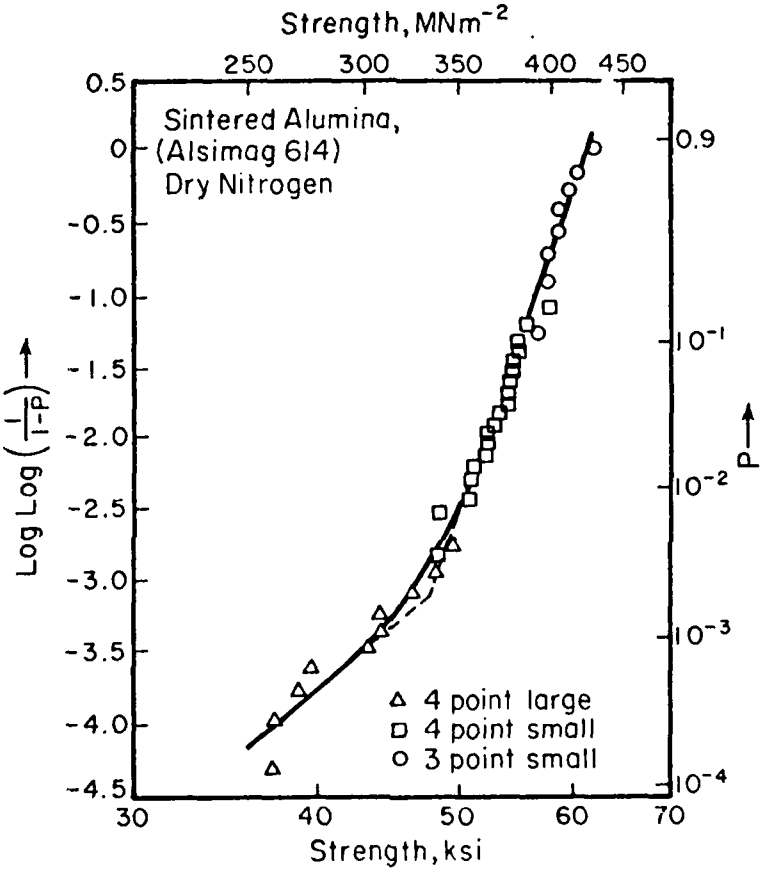

FIGURE B-4.

FIGURE B-4. Weibull plot of the data obtained on three different sizes of an alumina ceramic tested in dry nitrogen. Failure probabilities for the small and large 4-point bend data have been normalized to those of the small 3-point bend specimen (Ref. 16, 17).

variations of K_{IC} have been found in recent strength analyses of a hot-pressed alumina[6] and a hot-pressed silicon nitride[18]. In the case of the alumina ceramic, K_{IC} increased with the extent of slow crack growth that preceded fracture. The analysis of the silicon nitride ceramic has not yet been sufficient to establish whether the K_{IC} variation is random or a function of failure stress.

The method used to detect these specimen-to-specimen variations in K_{IC} utilized a feature on the fracture surface known as a "mirror"[4]. This is a rather readily observable flat circular region that surrounds the Griffith crack. The radius of the mirror, r, depends on the stress at which the specimen fractures, such that:

$$\sigma_f \sqrt{r} = 2.35 K_{IC} . \qquad \text{(B-13)}$$

Thus, K_{IC} can be evaluated for individual strength-tested specimens by supplemental measurements of fracture-mirror radii.

Although not necessarily a complexity in describing strength, it has been demonstrated at least partially that dispersed strength values and a size dependence of strength are not inherent characteristics of ceramics. Strengths of glass-ceramic specimens of widely varying size exhibited no size dependence and small standard deviations ($\sim$3 percent) when failure was from extrinsic surface flaws[19]. No abnormal procedures were used in surface finishing the specimens, and the absence of a size dependence was observed in strength tests in which slow crack growth was present as well as absent. The ceramic, however, contained a sparse population of pores which were responsible for some low-stress failures, and there was a size dependence when pore failures were represented in the strength data. The absence of a size dependence indicates a very large Weibull modulus, evaluated to be greater than 50 for the surface flaw failures.

CONCLUSIONS

The product of tensile stress and crack severity, $\sigma_t s = K_I$, determines whether a ceramic structural member will fail by brittle fracture. Failure occurs when $K_I = K_{IC}$ at any site in the component.

K_I can increase with time under stress due to slow crack growth, yet remain subcritical. Strength degradation from slow crack growth is predictable providing that K_{IC} and crack shape are unaffected by the growth. Knowledge of the empirical slow crack growth parameters, A and n, is required for the prediction.

Crack severity, s, in the ceramic depends on small intrinsic or extrinsic flaws, or both, which intensify stress locally. Because of an inhomogeneous population of worst flaws, strengths of identical ceramic specimens tested alike are usually dispersed, precluding assignment of an unique strength value to a ceramic and giving rise to a size and stress-distribution dependency of strength.

Statistical formulations derived by Weibull are available for providing a mathematical description that can be used to predict effects of size or stree-distribution on a ceramic's strength. Use of Weibull's formulations requires an experimentally determined strength dispersion(s) to evaluate descriptive parameters, specifically the Weibull modulus, m, and a normalizing constant, σ_0. The stress, σ_u, corresponding to a zero probability of failure may also be required to describe strength.

In using the statistical approach, strength is defined in terms of the probability, P, of failure at a given stress, and the component is designed on the basis of an acceptable failure probability. The P-σ relation for a ceramic component can be obtained regardless of the component's size or the stress distribution in it when an applicable Weibull formulation is available for the material, but the failure stress range for the component is limited to the range covered by experimental data. Applicability of a Weibull formulation to de-

signing a component also requires that the experimental data on which it is based meet stringent demands, particularly with respect to precision and similarity of the flaw population responsible for failure.

Investigations has shown that mathematical descriptions of ceramic P-σ relations can be complicated by the presence of more than one population of "worst" flaws and by variability of K_{IC}.

Strength analyses in which time and size effects on fracture strengths are defined for conditions encountered are required in order to specify the best ceramic for a given structural application.

Appropriate proof testing of each component can provide positive assurance of structural integrity.

REFERENCES
ON
STRUCTURAL DESIGNING WITH CERAMIC MATERIALS

(1) Griffith, A. A., Phil. Trans. R. Soc., A221, 163-198 (1920).

(2) Bansal, G. K., J. Am. Ceram. Soc., 59 [1-2] 87-88 (1976).

(3) Brown, Jr., W. F. and Srawley, J. E., Am. Soc. Test, Mater., Spec. Tech. Publ., No. 410, 1-15 (1967).

(4) Bansal, G. K., Phil. Mag. 35, [4] 935-44 (1977).

(5) Hubner, H. and Jillek, W., J. Mat. Sc., 12 117 (1977).

(6) Bansal, G. K. and Duckworth, W. H., "Comments on Subcritical Crack Extension and Crack Resistance in Polycrystalline Alumina", accepted for publication in J. Mat. Sc (1977).

(7) Freiman, S. W., Williams, A., Mecholsky, J. J., and Rice, R. W., pp 824-34 in Ceramic Microstructures' 76, edited by R. M. Fulrath and J. A. Pask, Westview Press, Boulder, Colorado (1977).

(8) Bansal, G. K., pp 860-71, in ibid.

(9) Evans, A. G. and Lange, F. F., J. Mat. Sc., 10 [10] 659-65 (1975).

(10) Wiederhorn, S. M., in Fracture Mechanics of Ceramics, edited by Bradt, Hasselman, and Lange, pp 613-46, Plenum Press, New York (1973).

(11) Evans, A. G. and Johnson, H., J. Mat. Sc. 10, 214-22 (1975).

(12) Bansal, G. K. and Duckworth, W. H., "Effects of Moisture-Assisted Slow Crack Growth on Ceramic Strengths", accepted for publication in J. Mat. Sc. (1977).

(13) Davies, D.G.S., Proc. Br. Ceram. Soc., 22 pp 429-52 (1973).

(14) Evans, A. G. and Wiederhorn, S. M., Int. J. Fract., 10 [3] 379-92 (1974).

(15) Weibull, W., J. Appl. Mech. 18 [3] 293-97 (1951).

(16) Johnson, C. A. and Prochazka, S., "Investigation of Ceramics for High-Temperature Components", Quarterly Progress Report #3, prepared for Naval Air Development Center under Contract No. N62269-76-C-0243 (January, 1977).

REFERENCES
(Continued)

(17) Bansal, G. K., Duckworth, W. H., and Niesz, D. E., J. Am. Ceram. Soc. 59 [11-12] 472-78 (1976).

(18) Bansal, G. K. and Duckworth, W. H., unpublished research.

(19) Bansal, G. K., Duckworth, W. H., and Niesz, D. E., Bull., Am. Ceram. Soc., 55 [3] 289-92, 307 (1976).

Unclassified

SECURITY CLASSIFICATION OF THIS PAGE (When Data Entered)

REPORT DOCUMENTATION PAGE

READ INSTRUCTIONS BEFORE COMPLETING FORM

1. REPORT NUMBER: Final Report	2. GOVT ACCESSION NO
3. RECIPIENT'S CATALOG NUMBER	
4. TITLE (and subtitle): Strength Analysis of Brittle Materials.	5. TYPE OF REPORT & PERIOD COVERED: FINAL rept. Apr. 73 - Oct. 77,
	6. PERFORMING ORG. REPORT NUMBER
7. AUTHOR(s): G. K. Bansal, W. H. Duckworth, D. E. Niesz	8. CONTRACT OR GRANT NUMBER(s): N00014-73-C-0408 NR 032-541
9. PERFORMING ORGANIZATION NAME AND ADDRESS: Battelle Columbus Laboratories 505 King Avenue Columbus, Ohio 43201	10. PROGRAM ELEMENT, PROJECT, TASK AREA & WORK UNIT NUMBERS
11. CONTROLLING OFFICE NAME AND ADDRESS	12. REPORT DATE: 11 Nov. 77
	13. NUMBER OF PAGES: 66 + 269 F.
14. MONITORING AGENCY NAME & ADDRESS (if different from Controlling Office): Dr. Arthur M. Diness	15. SECURITY CLASS (of this report): Unclassified
	15a. DECLASSIFICATION/DOWNGRADING SCHEDULE

16. DISTRIBUTION STATEMENT (of this Report)

Reproduction in whole or in part is permitted for any purpose of the United States Government.

17. DISTRIBUTION STATEMENT (of the abstract entered in Block 20, if different from Report)

18. SUPPLEMENTARY NOTES

Important results of the research are given in two separate publications attached as appendices A and B of this report.

19. KEY WORDS (Continue on reverse side if necessary and identify by block number)

Ceramic strength behavior, size-strength relations, brittle fracture, strength theories, Griffith's Fracture criterion, Weibull statistics, critical flaw size, critical stress-intensity factor, fracture surface energy.

20. ABSTRACT (Continue on reverse side if necessary and identify by block number)

Fracture stresses in specimens of four commercial polycrystalline ceramics differing in each linear dimension by a factor of four or five were measured at room temperature under controlled conditions. Data obtained were analyzed with the aid of fractographic examinations for applicability of Weibull statistics.

407 D

DD FORM 1473 EDITION OF 1 NOV 65 IS OBSOLETE

SECURITY CLASSIFICATION OF THIS PAGE (When Data Entered)

20. ABSTRACT (Continued)

A central problem in attempting to use ceramic materials in demanding structural applications is uncertainty about the stresses to which they can be safely subjected. A ceramic rarely, if ever, exhibits a characteristic failure stress. This stress depends on the nature and distribution of microscopic flaws that intensify stress locally, and fracture initiates at a single "worst" flaw when Griffith's criterion for crack instability is met. Within the basic framework, theories are available for treating effects of time, size, and stress distribution on failure stress. This paper reviews these theories, and discusses their use in specifying limiting stresses in designing structural members.